

Resveratrol inhibits transforming growth factor- β -induced proliferation and differentiation of ex vivo human lung fibroblasts into myofibroblasts through ERK/Akt inhibition and PTEN restoration

Evelina Fagone,¹ Enrico Conte,¹ Elisa Gili,¹ Mary Fruciano,¹ Maria Provvidenza Pistorio,¹ Debora Lo Furno,² Rosario Giuffrida,² Nunzio Crimi,¹ and Carlo Vancheri¹

¹Department of Internal Medicine and Medical Specialities, University of Catania, Catania, Italy

²Department of Physiological Sciences, University of Catania, Catania, Italy

ABSTRACT

The authors investigated the role of resveratrol (RV), a natural polyphenolic molecule with several biological activities, in transforming growth factor- β (TGF- β)-induced proliferation and differentiation of ex vivo human pulmonary fibroblasts into myofibroblasts. The effects of RV treatment were evaluated by analyzing TGF- β -induced α -smooth muscle actin (α -SMA) expression and collagen production, as well as cell proliferation of both normal and idiopathic pulmonary fibrosis (IPF) lung fibroblasts. Results demonstrate that RV inhibits TGF- β -induced cell proliferation of both normal and pathological lung fibroblasts, attenuates α -SMA expression at both the mRNA and protein levels, and also inhibits intracellular collagen deposition. In order to understand the molecular mechanisms, the authors also investigated the effects of RV treatment on signaling pathways involved in TGF- β -induced fibrosis. The authors show that RV inhibited TGF- β -induced phosphorylation of both extracellular signal-regulated kinases (ERK1/2) and the serine/threonine kinase, Akt. Moreover, RV treatment blocked the TGF- β -induced decrease in phosphatase and tensin homolog (PTEN) expression levels.

KEYWORDS AKT, ERK1/2, human lung fibroblasts, IPF, myofibroblasts, PI3K, PTEN, resveratrol, TGF- β

Fibroblasts are the predominant secretory cells of extracellular matrix (ECM) proteins in the lung and also are key mediators of normal and pathological lung remodeling. In idiopathic pulmonary fibrosis (IPF)/usual interstitial pneumonia (UIP), fibroblasts proliferate and can differentiate into myofibroblasts, which are characterized by α -smooth muscle actin (α -SMA) expression and increased generation and secretion of ECM proteins (i.e., collagen and fi-

bronectin) that contribute to fibrotic disorders [1–4]. Under normal circumstances, such as in wound healing, myofibroblasts undergo apoptosis in the wound site after healing is complete. In contrast, in the absence of apoptosis, the prolonged presence of myofibroblasts leads to an overproduction of ECM proteins. In IPF/UIP, the presence and persistence of myofibroblasts are believed to be a key element in the development of fibrosis. Myofibroblast differentiation is controlled by a complicated network that consists of cytokines, chemical mediators, growth factors, and oxygen radicals derived from inflammatory cells [3, 5]. Nevertheless, transforming growth factor (TGF)- β seems to play a central role in this process, as it is a potent paracrine mediator of differentiation and also contributes to the development of pulmonary fibrosis following the expansion of lung myofibroblasts [6–8]. Among the signaling pathways triggered by TGF- β , mitogen-activated

Received 19 May 2010; accepted 8 September 2010

Evelina Fagone and Enrico Conte contributed equally to this work. The research has been funded by the European Community's Seventh Framework Programme (FP7/2007–2013) under grant agreement HEALTH-F2-2007-202224 eurIPFnet. The authors are indebted to Dr. Enrico Potenza, Head of Thoracic Surgery Section of Garibaldi Hospital, Catania Italy, for supplying the necessary lung specimens. Address correspondence to Dr. Enrico Conte or Dr. Carlo Vancheri, Department of Internal Medicine and Medical Specialities, University of Catania, via S. Sofia 78, Catania, 95123 Italy. E-mail: econte@unict.it; vancheri@unict.it

protein kinase (MAPK)/extracellular signal-regulated kinase 1/2 (ERK1/2) activation has been shown to be involved in TGF- β -induced phenotypic transformation of human lung fibroblasts into myofibroblasts [9–11]. Furthermore, phosphoinositide 3-kinase (PI3K)/Akt, which regulates a wide variety of cellular processes, including cell proliferation, metabolism, migration, and survival, is also involved in the establishment of fibrotic fibroblasts by opposing the functions of phosphatase and tensin homolog (PTEN) [12–14]. In fact, PTEN has been implicated in myofibroblast differentiation based on 3 main observations. First, a distinct inhibition or loss of PTEN expression in fibroblasts correlates with α -SMA expression in lung biopsy samples from patients with IPF/UIP. Second, in vitro myofibroblast differentiation has been shown to be inhibited by PTEN. Finally, recent studies have demonstrated that the in vivo inhibition of PTEN promotes fibrosis.

Several features of myofibroblast differentiation have been previously described, although mechanisms that inhibit or reverse this process are not as well understood. Currently, established therapies with anti-inflammatory (i.e., prednisone) and immunosuppressive (i.e., azathioprine, ciclofosamide) drugs do not block fibrosis in IPF/UIP [15]. Although clinical trials have also investigated the potential benefits of other molecules, it is critical to develop new therapeutic agents that block the activation, proliferation, and transition of myofibroblasts as well as ECM deposition [16].

Resveratrol (RV; *trans*-3,4',5-trihydroxystilbene) is a polyphenolic molecule found in the skin of grapes, peanuts, mulberries, and red wine. A recent study has shown that the antioxidant properties of RV exert an in vivo protective role in bleomycin-induced pulmonary fibrosis by attenuating oxidative injury and fibrosis [17]. Several biological activities have been attributed to RV, such as antioxidant, vasorelaxant, antiplatelet, anti-inflammatory, anticancer, and estrogenic agent [18–22]. RV has also been shown to possess a protective role in various cardiovascular diseases by reducing atherosclerosis and attenuating reperfusion-mediated damage following myocardial ischemia [23]. Furthermore, RV is also able to inhibit vascular smooth muscle cell remodeling as well as the growth and proliferation of cardiac fibroblasts [24].

In this study, RV is shown to suppress TGF- β -induced cell proliferation and differentiation of human pulmonary fibroblasts into myofibroblasts. RV treatment of fibroblast cells inhibited the expression of α -SMA at both the mRNA and protein levels and also attenuated collagen deposition. Addition-

ally, RV treatment is also shown to inhibit TGF- β -induced phosphorylation of ERK1/2 and Akt, but increase PTEN levels despite reduction by TGF- β . Taken together, these results suggest that RV may exert antifibrotic properties in the human lung by limiting fibroblast proliferation and myofibroblast differentiation.

MATERIALS AND METHODS

Fibroblast Cultures

Primary cell lines of human adult lung fibroblasts were established according to the method previously described by Jordana and coworkers [25]. Outgrowths were derived from IPF/UIP patient biopsies ($n = 5$; their ages ranged from 52 and 61 years, 3 of the 5 patients were men) or from histologically normal areas of surgical lung specimens from matched patients undergoing cancer-related surgeries ($n = 5$). Prior to treatment, cells were incubated for 24 hours in serum-free medium, then treated with RV (1–20 μ M; Sigma) 30 minutes before subsequent TGF- β stimulation and/or with TGF- β (10 ng/mL; Chemicon). Afterward, cells were incubated for 48 hours in serum-free medium, and then trypsinized. All of the phenotypic and functional parameters were then evaluated. In some experiments, cells were treated with RV 24 hours after TGF- β stimulation.

Evaluation of Cell Proliferation

Cell numbers were determined by counting cells on a hemocytometer (Burker chamber) after trypan blue staining. A mean of 4 fields was used to calculate the average number of cells. Cell proliferation was also evaluated by using the WST-1 kit (Roche, Basel, Switzerland). Briefly, after the specified treatment, cells were exposed to WST-1 for 1 hour at 37°C. The formation of WST-1 formazan was spectrophotometrically monitored using a reference wavelength of 480 nm. Additionally, the CellTrace CFSE Cell Proliferation Kit (Molecular Probes) was used according to manufacturer's instructions. Briefly, cells were stained with the fluorescent compound, carboxyfluorescein succinimidyl (CFSE; 2.5 μ M), prior to being plated, and then analyzed by flow cytometry following the specified treatments.

Measurement of Collagen Protein Levels

Fibroblasts were grown in 6-well plates until they reached 50% confluency. The culture medium was

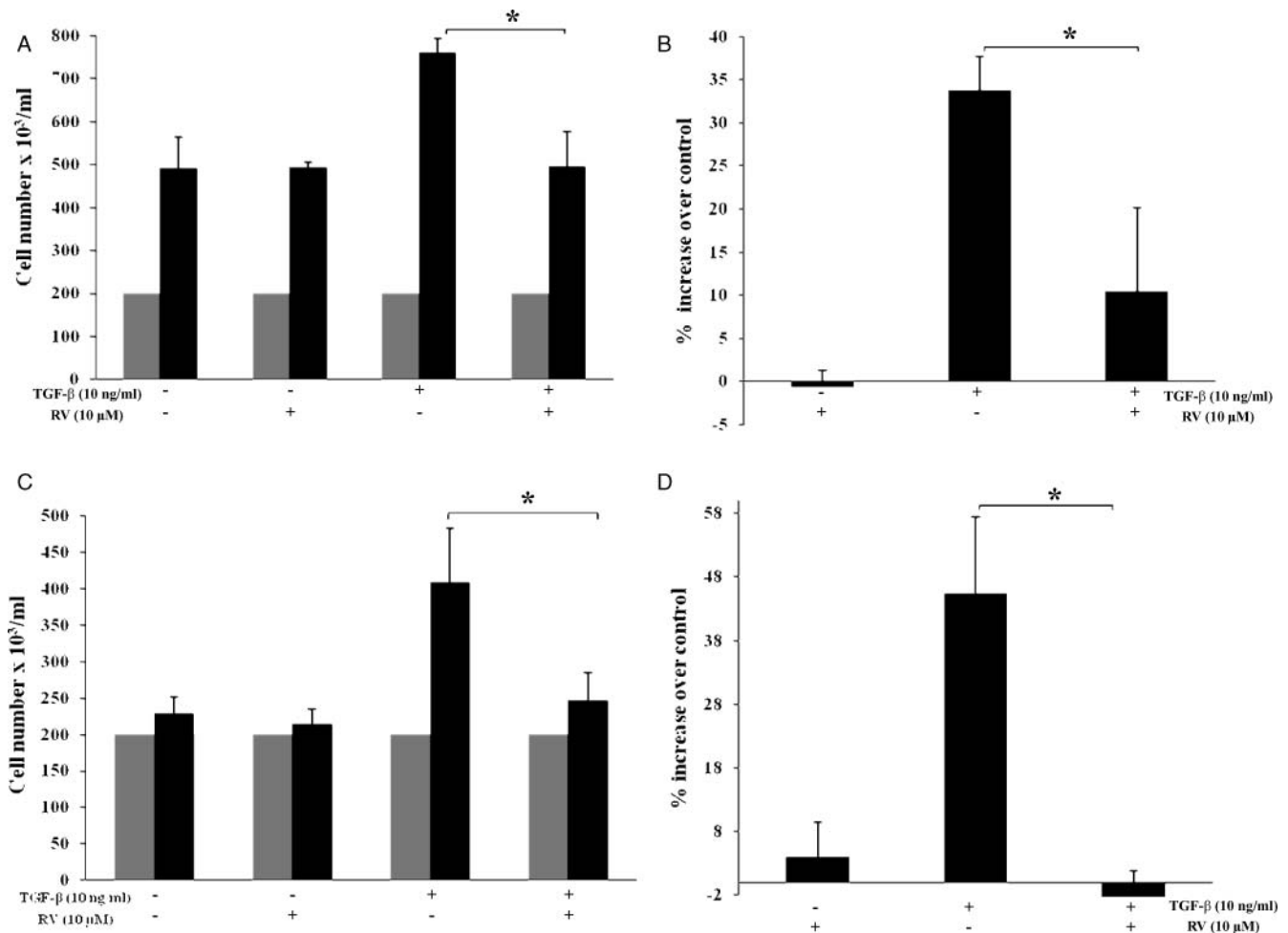


FIGURE 1 Antiproliferative effect of RV in primary human lung fibroblasts stimulated with TGF- β . Ex vivo human lung fibroblasts isolated from normal lung areas or obtained from IPF patient biopsies ($n = 5$ for both) were plated in 6-well dishes at a density of 2×10^5 /mL in supplemented RPMI medium ($t = 0$). After 2 days of culture, cells were serum starved for 24 hours, treated with or without RV ($10 \mu\text{M}$) for 30 minutes, then incubated with or without TGF- β (10 ng/mL) for 48 hours in serum-free medium ($t = 48$ hours). **(A)** Normal fibroblast counts determined by optical microscopy; gray bars represent $t = 0$ and black bars represent $t = 48$ hours. **(B)** WST-1 cell proliferation assay with normal fibroblasts; the percentage of absorbance (Ab) increase, relative to the control, was calculated as $[(\text{Ab of treated cells}/\text{Ab of control cells}) \times 100] - 100$. **(C)** IPF fibroblast counts determined by optical microscopy. **(D)** WST-1 cell proliferation assay with IPF fibroblasts. All measurements were performed in triplicate. Mean values and standard deviation (SD) of 5 independent experiments are reported. Asterisks indicate a P value $< .05$.

then removed and the cells were washed twice before incubation in serum-free RPMI medium for 24 hours. Afterward, the cells were treated with RV ($10 \mu\text{M}$) for 30 minutes in serum-free medium and then stimulated with TGF- β (10 ng/mL). Collagen levels were measured at 24, 48, and 72 hours following TGF- β stimulation. Total soluble collagen was measured in cellular lysates using the Sycrol Soluble Collagen Assay (Biocolor, Newtownabbey, Northern Ireland) according to the manufacturer's instructions. Briefly, 1 mL of Sycrol Dye Reagent was added to 100 μL cellular lysate and mixed by

inverting the reaction for 30 minutes at room temperature in a mechanical shaker. The collagen-dye complex was precipitated by centrifugation at $10,000 \times g$ for 1 minute. The unbound dye solution was removed by carefully inverting the samples. Any remaining dye droplets were removed by gently tapping the inverted tube on a paper tissue. The precipitated complex was resuspended in 1 mL of alkaline reagent. The resulting solution was finally added to a 96-well flat bottom plate and read on a plate reader with an absorbance wavelength of 540 nm. The samples were evaluated relatively to standard curves

obtained with the collagen control provided by the kit's manufacturer.

RNA Extraction, Reverse Transcription, and Quantitative Real-Time Polymerase Chain Reaction (PCR)

Total RNA from cells was extracted using Trizol Reagent (Invitrogen, Paisley, UK), quantified by spectrophotometrical analysis with BIO-photometer (Eppendorf, Germany) and treated with DNase (Invitrogen). The generation of cDNA from RNA was performed with Superscript II Reverse Transcriptase (RT; Invitrogen) and random hexamer primers (Invitrogen), according to the manufacturer's instructions. Quantitative real-time PCR of cDNAs was per-

formed using the IQ SYBR Green Supermix (Qiagen, Germany) in conjunction with commercially available *ACTA2*, *PTEN*, and glyceraldehyde 3-phosphate dehydrogenase (*GAPDH*) primers (Qiagen), according to the manufacturer's instructions. Amplification conditions for each of the genes were as follows: DNA denaturation at 94°C for 5 minutes followed by 45 cycles of 2 steps of 95°C for 15 sec and 60°C for 30 sec. Relative quantification of target gene levels was performed by comparing ΔC_T , as previously described [26].

Flow Cytometry Analysis

Cells were washed in phosphate-buffered saline (PBS)/1% bovine serum albumin (BSA), fixed with 2% paraformaldehyde (PFA) for 20 minutes at 4°C,

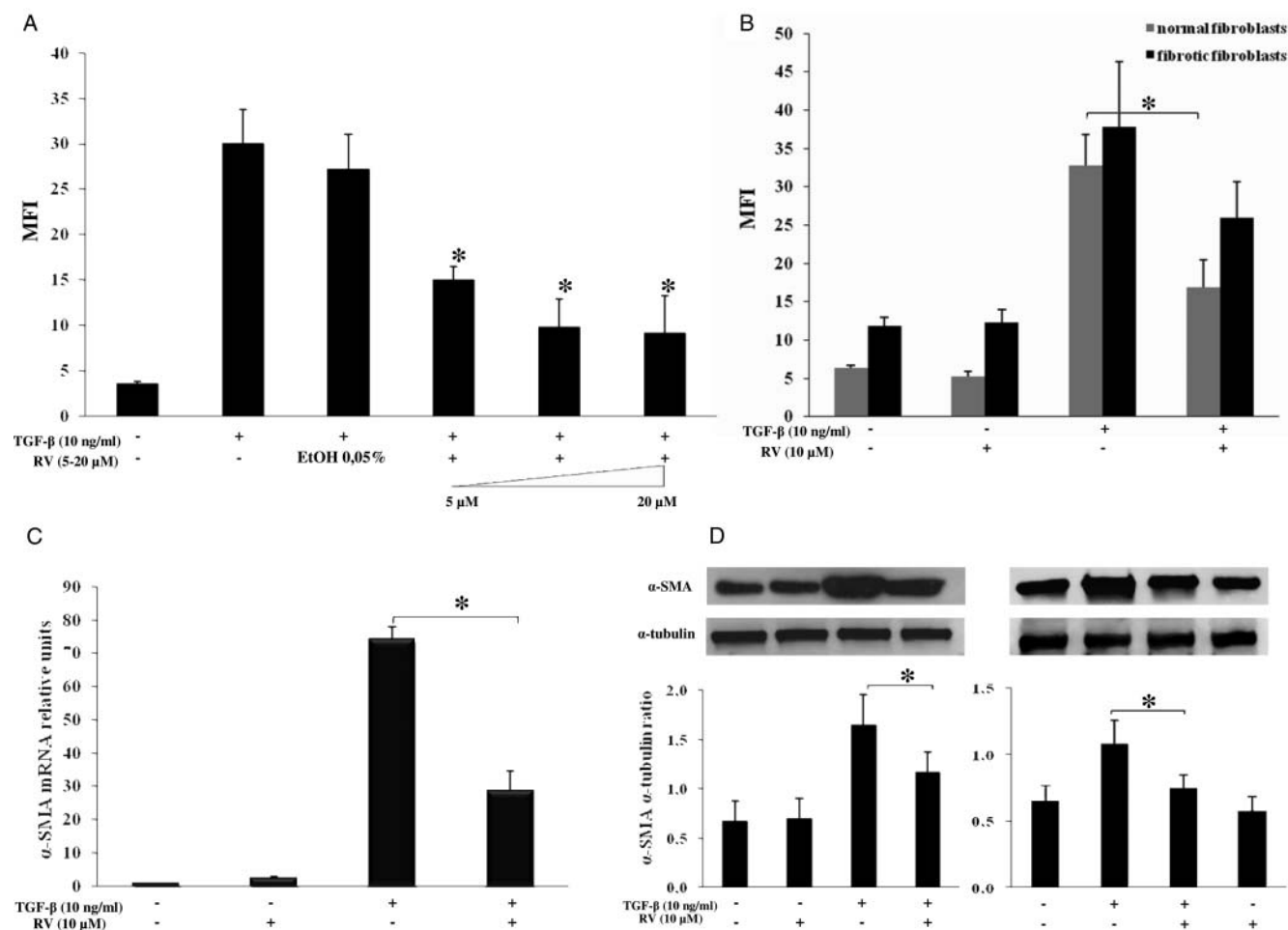


FIGURE 2 Inhibitory effects of RV treatment on TGF- β -induced α -SMA expression in ex vivo human lung fibroblasts. Analysis of α -SMA expression in normal and IPF pulmonary fibroblasts grown and treated as illustrated in Figure 1. The flow cytometry values of mean fluorescence intensity (MFI) are reported in the graphs shown in **A** and **B**. Quantitative real-time PCR data are shown in **C**. Representative Western blots with pertinent densitometric analysis are shown in **D** (normal cells on the left side and IPF cells on the right). Mean values and SD of at least 3 independent experiments with different cell lines are shown. Statistical significance ($P < .05$) is indicated with an asterisk.

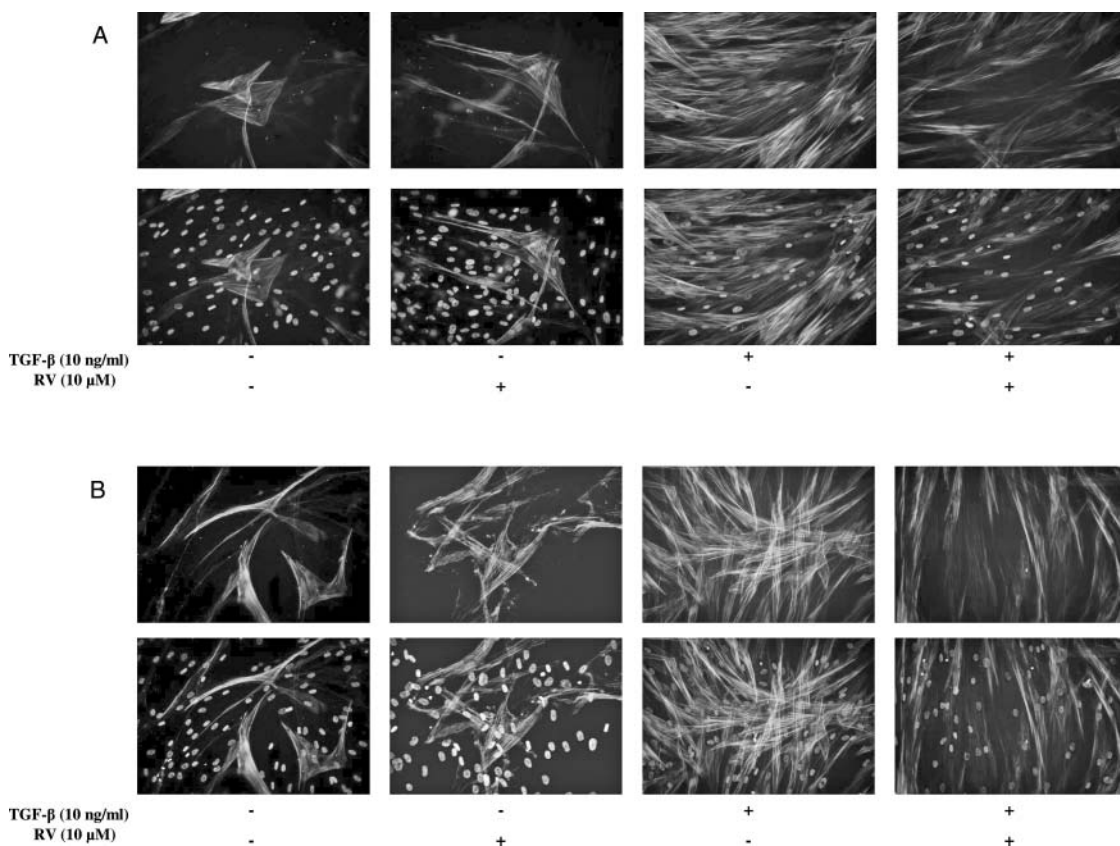


FIGURE 3 RV treatment prevents TGF- β -induced α -SMA fiber deposition. Normal (**A**) and IPF (**B**) fibroblasts were grown and treated as illustrated in Figure 1. The cells were fixed and incubated overnight with the primary antibody, anti- α -SMA, and then incubated with the secondary antibody, goat F(ab')₂ fragment anti-mouse IgG (H+L)-FITC as well as with DAPI. Digital images were acquired using a fluorescence microscope coupled to a digital camera ($\times 20$ magnification). Representative pictures obtained with the FITC filter are shown in upper part of each panel, whereas DAPI images to show cell nuclei were superimposed in the lower part. Similar results were obtained in 3 independent experiments.

and then permeabilized with $1\times$ Triton (Sigma-Aldrich) for 5 minutes at 4°C . Afterward, cells were washed once with PBS/1% BSA and incubated with anti- α -SMA antibody (Ab) (1:100; Dako) for 60 minutes at room temperature. Then, the cells were washed once with PBS/1% BSA and incubated with goat F(ab')₂ fragment anti-mouse immunoglobulin G (IgG) (H+L)-fluorescein isothiocyanate (FITC) (1:1000) (Beckman Coulter) for 60 minutes at room temperature in the dark. For the CFSE assay, a standard fixation protocol (3.7% formaldehyde for 15 minutes at room temperature) was used. Samples were analyzed using a Coulter Epics Elite ESP flow cytometer (Coulter, Miami, FL, USA). A minimum of 10,000 forward and side scatter gated events were collected per specimen. Samples were excited at 488 nm and fluorescence was monitored at 525 nm. Fluorescence was collected using logarithmic amplification. Mean fluorescence intensity (MFI) values were calculated and recorded automatically.

Western Blot Analysis

Cultured cells were lysed in a solution of 10 mM EDTA, 1% Triton X-100, 1 mM phenylmethylsulfonylfluoride (PMSF), and 15 $\mu\text{L}/\text{mL}$ Protease Inhibitor Cocktail (all from Sigma-Aldrich). Protein concentrations were determined by the Bradford method using an aliquot of the sample. Samples were then diluted in sample buffer and boiled for 5 minutes. Electrophoresis was performed on a 12% sodium dodecyl sulfate-polyacrylamide gel electrophoresis (SDS-PAGE) gel (40 mA/h) using 60 μg of protein/lane. After electrophoresis, proteins were transferred onto a nitrocellulose membrane (Hybond ECL; Amersham Biosciences Europe, Milan, Italy) for 2 hours at room temperature with a transblot semidry transfer cell. After BSA blocking, membranes were incubated overnight at 4°C with: monoclonal mouse anti- α -SMA Ab (1:500; Dako Cytomation, Denmark), mouse anti-PTEN Ab (1:500; Cell

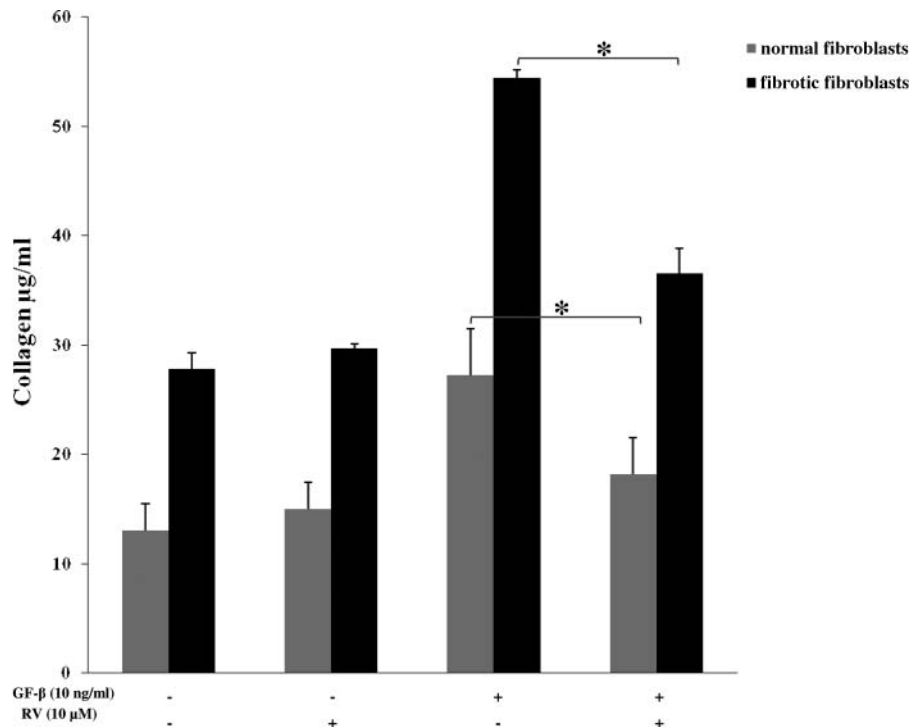


FIGURE 4 RV treatment inhibits TGF- β -induced collagen deposition. Normal and IPF fibroblasts were grown and treated as illustrated in Figure 1. Collagen levels were then evaluated after 48 hours of incubation. Total soluble collagen was measured in cellular lysates with the Syrcol Soluble Collagen Assay, as detailed in Materials and Methods. Mean values and SD of 3 independent experiments for both normal and pathological fibroblasts are reported in gray and black bars, respectively. Asterisks indicate statistically significant values ($P < .05$).

Signaling Technology, Beverly, MA, USA), rabbit anti-ERK and rabbit anti-p-ERK, which recognize both ERK1 and ERK2 as well as p-ERK1 and p-ERK2, respectively (1:1000; Cell Signaling Technology), as well as rabbit anti-Akt and rabbit anti-p(Ser⁴⁷³)-Akt (1:200; Cell Signaling Technology). Membranes were then thoroughly washed and incubated with horseradish peroxidase-conjugated anti-mouse or anti-rabbit secondary antibodies (1:5000; Santa Cruz Biotechnology, Santa Cruz, CA, USA). Specific bands were visualized using the SuperSignal chemiluminescent detection system (Pierce Chemical, Rockford, IL, USA).

Immunocytochemistry Analysis

Immunocytochemistry was carried out in culture dishes of pulmonary fibroblasts. Cells were first washed with PBS, fixed with 4% PFA for 30 minutes, and then permeabilized with 0.2% Triton X-100 (Sigma-Aldrich). Afterward, cells were incubated for 30 minutes with a 5% solution of normal goat serum (Sigma-Aldrich) and then incubated overnight

at 4°C with anti- α -SMA (1:100; Dako Italia, Milan, Italy). The following day, cells were washed with PBS and incubated for 1 hour at room temperature with goat F(ab')₂ fragment anti-mouse IgG (H+L)-FITC (1:200; Beckman Coulter, Milan, Italy). Cells were then washed with PBS, and incubated with 4'-6-diamidino-2-phenylindole (DAPI) (1:10,000; Invitrogen). As a control, the specificity of immunostaining was checked by omitting incubation with the primary antibody. Digital images ($\times 20$ magnification) were acquired using a Leica DMRB fluorescence microscope that is coupled to a Nikon digital camera.

Statistical Analysis

Statistical significance across treatment groups was determined using either a one-way analysis of variance (ANOVA) with Tukey's multiple-comparison test or by a t test using Statgraphic Centurion XV (StatPoint Technologies, ADALTA, Italy) software. A P value $< .05$, which indicates a statistically significant difference, is designated with a single asterisk.

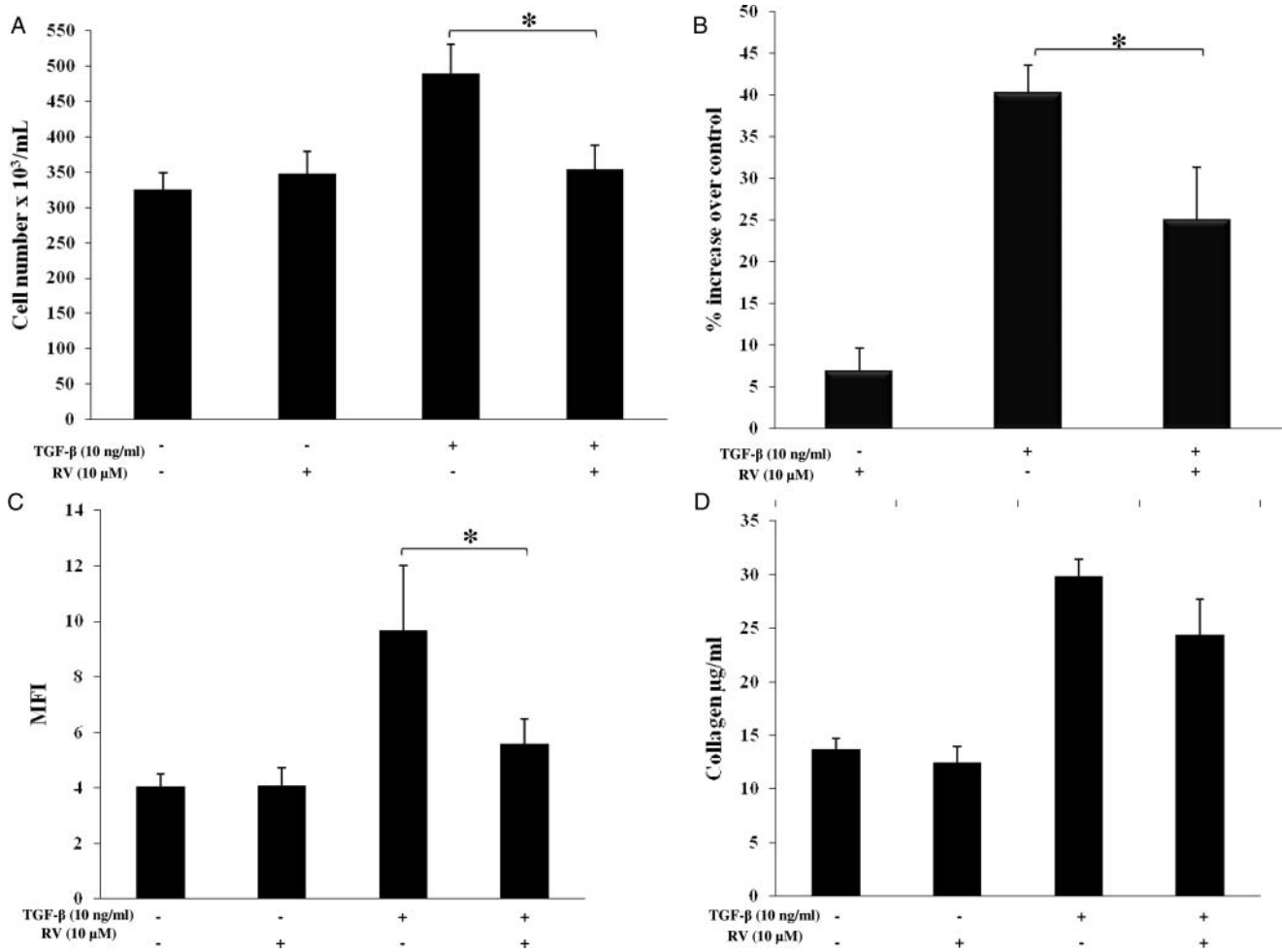


FIGURE 5 Effects of RV treatment on normal lung fibroblasts 24 hours after TGF- β stimulation. Normal lung fibroblasts were plated in 6-well dishes at a density of 2×10^5 /mL in supplemented RPMI medium. Forty-eight hours later, the cells were serum starved for 24 hours and then incubated with or without TGF- β (10 ng/mL) in serum-free medium. After 24 hours, the cells were then treated with or without RV (10 μ M), cultured for an additional 24 hours and then collected for analysis. Cell count by optical microscopy is shown in **A**. Results of WST-1 cell proliferation assay (% increase relative to control) are reported in **B**. **C** shows α -SMA levels determined by flow cytometry (MFI values) and **D** shows total soluble collagen values determined by Syrcol assay. Mean values and SD of 5 independent experiments with 3 different cell lines are reported. Asterisks indicate statistically significant values ($P < .05$).

RESULTS

RV Treatment Abrogated TGF- β -Induced Proliferation of Primary Human Lung Fibroblasts

Ex vivo human pulmonary fibroblasts isolated from normal lung tissue or from IPF biopsies were cultured in vitro and before experiments starved for 24 hours in serum-free medium. The cells were then treated with RV (10 μ M) for 30 minutes, followed by stimulation with TGF- β (10 ng/mL) for 48 hours in serum-free medium. Untreated cells and cells treated with either RV or TGF- β alone served as controls. As shown in Figure 1, consistent with previous ob-

servations of Ramos *et al.* [7], the results obtained by WST-1 proliferation assay and cell counts performed by optical microscopy demonstrate that resting lung fibroblasts from IPF patients minimally proliferate in vitro, in contrast to fibroblasts from normal lung tissue that replicate actively. This phenomenon could lie in the fibroblast population heterogeneity, and in a major presence of terminally differentiated myofibroblasts in cultures of IPF fibroblasts compared to normal cells. However, fibrotic fibroblasts showed a slightly more robust proliferative response to TGF- β in comparison to normal cells. Interestingly, RV pretreatment abrogated TGF- β -induced proliferation in both normal and fibrotic fibroblasts, restraining cell numbers to basal levels. Results of

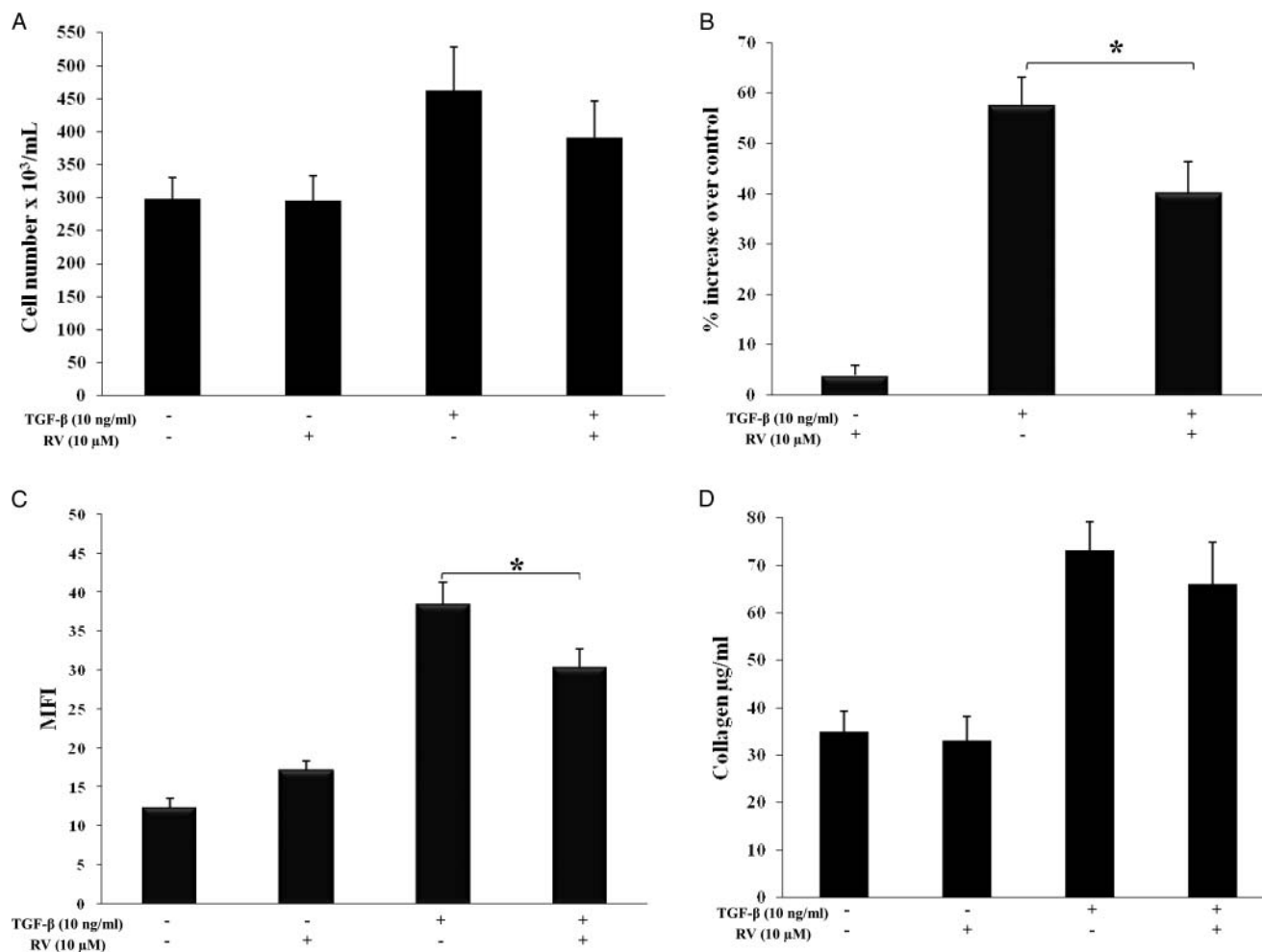


FIGURE 6 Effects of RV treatment on IPF lung fibroblasts 24 hours after TGF- β stimulation. IPF fibroblasts were plated in 6-well dishes at a density of 2×10^5 /mL in supplemented RPMI medium. Forty-eight hours later, the cells were serum starved for 24 hours and then incubated with or without TGF- β (10 ng/mL) in serum-free medium. After 24 hours, the cells were then treated with or without RV (10 μ M), cultured for an additional 24 hours and then collected for analysis. Cell count by optical microscopy is shown in **A**. Results of WST-1 cell proliferation assay (% increase relative to control) are reported in **B**. **C** shows α -SMA levels determined by flow cytometry (MFI values) and **D** shows total soluble collagen values determined by Sycrol assay. Mean values and SD of 5 independent experiments with 3 different cell lines are reported. Asterisks indicate statistically significant values ($P < .05$).

CFSE assay confirmed these effects (data not shown). In further support of these results, in a separate set of experiments, also treatment of normal cells as well as IPF fibroblasts with RV (10 μ M) 24 hours after TGF- β stimulation resulted in inhibition of cellular proliferation (see Figures 5A–B and 6A–B, respectively).

Effects of RV Treatment on TGF- β -Induced α -SMA Expression

Expression of the cytoskeletal protein α -SMA is a hallmark of the myofibroblast phenotype, and α -SMA is considered to be a marker of ongoing fibroblast differentiation. Therefore, we analyzed α -SMA expression at both the mRNA and protein levels, and the

results are shown in Figures 2 and 3. As evaluated by flow cytometry analysis, RV pretreatment significantly reduced TGF- β -induced α -SMA expression in normal human pulmonary fibroblasts in a dose-dependent manner (Figure 2A). In addition, substantial inhibition of α -SMA expression was also observed in fibrotic cells (Figure 2B). Moreover, as measured by quantitative real time PCR, α -SMA mRNA high levels induced by TGF- β treatment (70 \times) in normal cells were significantly decreased by RV pretreatment (Figure 2C). Similarly, Western blot analysis demonstrated a significant inhibition of TGF- β -induced total protein increase in both normal and IPF cells pretreated with RV (Figure 2D). On the other hand, as shown in Figure 3, the RV inhibitory effect on TGF- β -induced intracellular deposition of α -SMA fiber is

clearly visible by immunocytochemistry in both normal and IPF fibroblasts. Furthermore, 24 hours after TGF- β stimulation, RV treatment of both normal and IPF cells also resulted in a significant inhibition of TGF- β -induced α -SMA expression (see Figures 5C and 6C, respectively).

Effects of RV Treatment on TGF- β -Induced Collagen Deposition

Collagen accumulation is another characteristic feature of myofibroblasts, which are commonly observed in lung fibrosis. Therefore, we examined the effect of RV treatment on TGF- β -induced collagen deposition using the Syrcol assay. As shown in Figure 4, relative to the control, the total collagen level more than doubled in normal and fibrotic TGF- β -stimulated fibroblasts. In contrast, RV pretreatment substantially abrogated this TGF- β -mediated effect, resulting in collagen levels that were only slightly elevated compared to basal levels. Additionally, also RV treatment of both normal and fibrotic cells 24 hours after TGF- β stimulation substantially inhibited TGF- β -induced collagen deposition (Figures 5D and 6D).

Effects of RV Treatment on TGF- β -Activated Signaling Pathways

TGF- β activates various signaling cascades by binding to distinct receptors that activate downstream effectors, such as Smad proteins, which induce transcription of target genes. However, several studies have demonstrated that TGF- β can also signal through other pathways that are independent of Smads. We next sought to unravel the molecular mechanisms that underlie RV inhibition of TGF- β -induced profibrotic effects in lung fibroblasts by determining whether RV affects the pathways that are involved in TGF- β -induced fibrosis. As shown in Figures 7 and 8A (left panel), respectively, TGF- β -induced phosphorylation of ERK1/2 and Akt was significantly inhibited by pretreatment with RV. Interestingly, also RV treatment 24 hours after TGF- β stimulation is able to inhibit Akt phosphorylation, as shown in Figure 8A (right panel). PTEN expression levels and PTEN activity are both inversely correlated with Akt phosphorylation, α -SMA expression, cell proliferation, and collagen production. Therefore, we also investigated whether RV alters PTEN expression levels. As shown in Figure 8B–D, following TGF- β stimulation, PTEN mRNA and protein levels were both significantly decreased. However, RV treatment (both before and after TGF- β stimulation) partially restored the PTEN basal levels.

DISCUSSION

Current therapies are not able to arrest ongoing fibrosis in IPF/UIP patients. Therefore, it is important to investigate new therapeutic agents that are able to block the activation and proliferation of myofibroblasts, which play an essential role in fibrotic disease. A recent *in vivo* study demonstrated that RV exerts a protective role in bleomycin-induced pulmonary fibrosis by attenuating oxidative injury and fibrosis [17]. In our *in vitro* studies, RV treatment of TGF- β -stimulated primary human lung fibroblasts resulted in a significant alteration of the growth and proliferation of the stimulated fibroblasts, their differentiation into the myofibroblast hypersecretory phenotype, and also the signaling pathways involved in this process. The antiproliferative effects of RV have been extensively investigated in various cancer cell lines, smooth muscle cells, and cardiac fibroblasts [19, 24, 27]. Consistent with the RV effects observed in those cell lines, we show that RV pretreatment abrogated the TGF- β induced proliferation of human lung fibroblasts isolated from normal lung areas as well as from IPF patient biopsies. Interestingly, we observed a different proliferation rate between fibroblasts from IPF patients that minimally proliferate *in vitro* and normal fibroblasts that replicate actively. Even though inconclusive results have been previously reported on proliferative characteristics of fibroblasts obtained from normal versus IPF lungs [7,28–30], our finding supports data of Ramos and coworkers [7]. Moreover, we demonstrate that also RV treatment of fibroblasts 24 hours after TGF- β stimulation inhibited cell proliferation in both normal and IPF fibroblasts. Previous studies have shown that RV treatment decreases α -SMA expression in cultured human liver myofibroblasts and rat cardiac fibroblasts [24, 31]. Our studies show that treatment of lung fibroblasts with RV (also 24 hours after TGF- β stimulation) significantly inhibited TGF- β -induced α -SMA expression, as well as collagen deposition. Taken together, these data suggest a potential therapeutic benefit of RV in a TGF- β -driven fibrotic process.

The precise molecular mechanism used by RV is not completely understood, and likely involves multiple intracellular targets. It has been demonstrated that resveratrol may bind to estrogen receptors, because of its structural similarity to other phytoestrogen, and some effects could be mediated by these members of the nuclear receptor superfamily, activating the transcription of estrogen-responsive target genes and interacting with other signaling pathways [32]. All these mechanisms may contribute to sex-specific differences in fibrotic processes that are observed in human heart and other diseases.

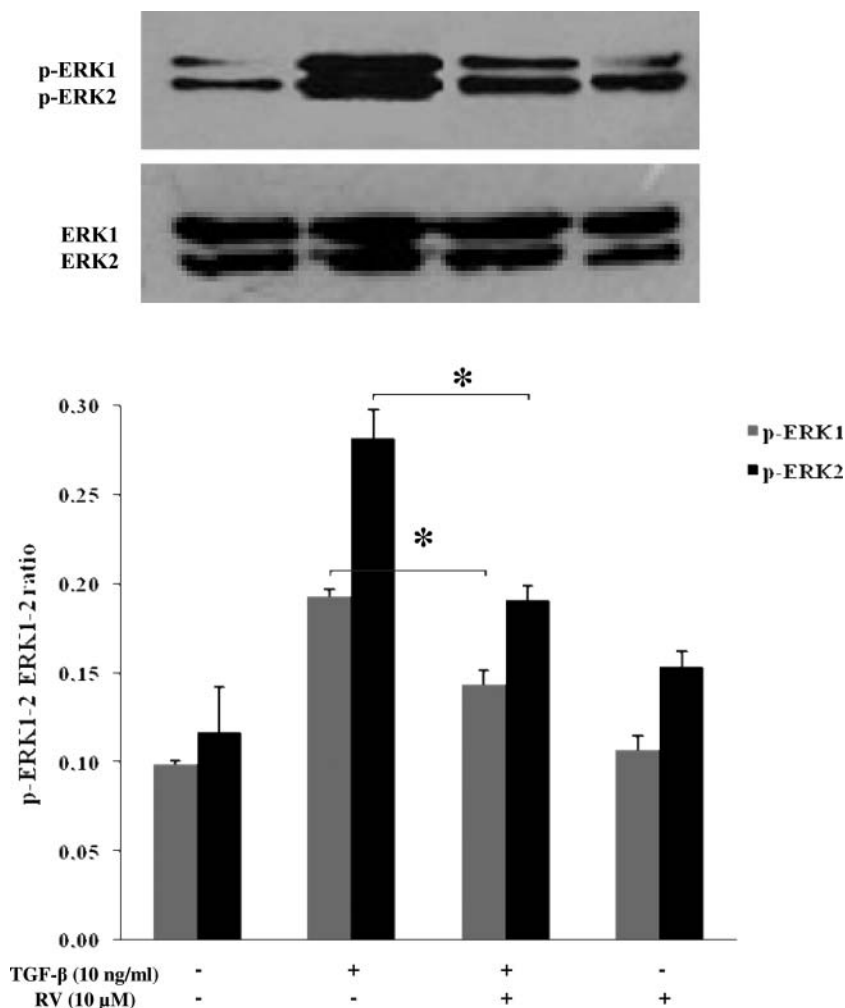


FIGURE 7 Effects of RV treatment on TGF- β -induced ERK1/2 activity. Representative Western blots of ERK and p-ERK proteins in ex vivo human lung fibroblasts. These blots demonstrate the effects of RV (10 μ M) pretreatment (30 minutes prior to TGF- β stimulation) on ERK1/2 phosphorylation (p-ERK1/2) after 15 minutes of TGF- β treatment (preliminary time course experiments demonstrated the strongest induction at this time point). As can be observed, total ERK levels did not change for any of the conditions tested, indicating equal protein loading among the samples. Densitometric analysis of normalized p-ERK levels for 3 independent experiments is shown in the lower panel. Asterisks indicate statistically significant values ($P < .05$).

Conversely, in this study we considered RV direct effects on TGF- β signaling pathways. TGF- β -mediated signaling cascades other than canonical Smad(s), such as MAPK/ERK1/2, are involved in TGF- β -induced phenotypic transformation of human lung fibroblasts into myofibroblasts [10]. Specifically, we have recently shown that the ERK1/2 pathway plays a specific role in this transformation process. On the other hand, ERK is known to be involved in the induction of α -SMA expression in TGF- β -treated human fetal lung fibroblasts [33]. The results presented in this study provide strong

evidence demonstrating RV-mediated inhibition of TGF- β -induced ERK1/2 phosphorylation. Our data are consistent with previous in vitro studies of rat vascular smooth muscle cells (VSMCs) [34] and rat cardiac fibroblasts [24] in which RV exhibits a dose-dependent reduction of ERK1/2 activation downstream from angiotensin II (Ang II) signaling. Interestingly, ANG II and TGF- β 1 may cooperate in the pathogenesis of pulmonary fibrosis [35]. Therefore the simultaneous inhibition of these pathways by RV could be efficacious in the treatment of fibrotic lung diseases.

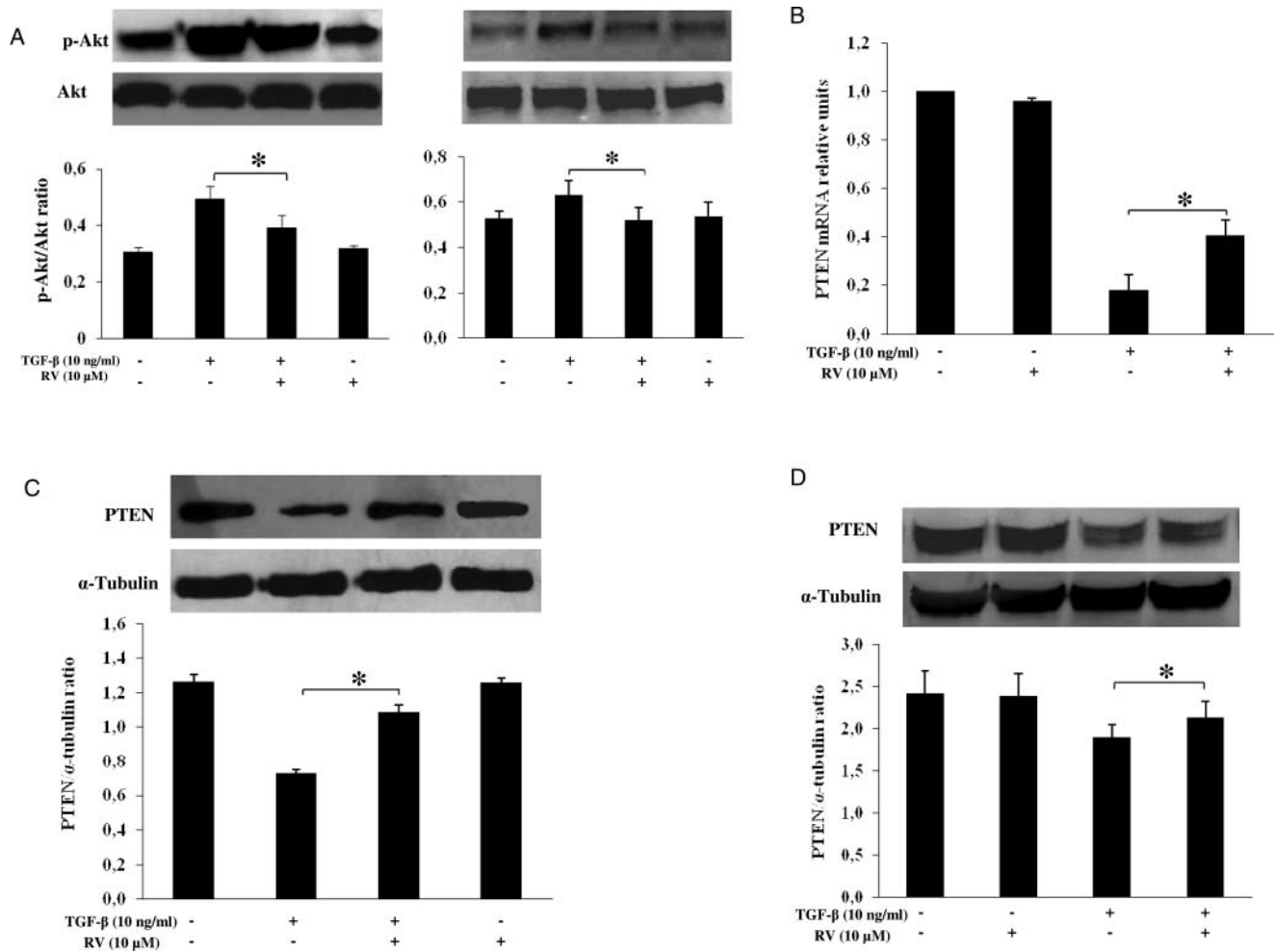


FIGURE 8 Effects of RV treatment on TGF- β -induced Akt activity and PTEN expression. Ex vivo normal human lung fibroblasts were grown and treated as illustrated in Figures 1 and 5. A strong TGF- β -induced Akt phosphorylation (p-Akt) after 24 hours of treatment is observed in a representative Western blot (shown in A, left side). This observation is paralleled by a dramatic drop in PTEN expression at both the mRNA (quantitative real-time PCR data shown in B) and protein levels (representative Western blot shown in C). However, RV pretreatment inhibited Akt activation and partially restored PTEN mRNA and protein levels (A–C). In a separate set of experiments, also RV treatment 24 hours after TGF- β stimulation was able to inhibit Akt phosphorylation (A, right side) and restore PTEN protein levels (D). Western blots are shown with densitometric analysis of normalized data collected from 3 independent experiments. Asterisks indicate statistically significant values ($P < .05$).

Through a multitude of protein targets, Akt is involved in various cellular processes such as proliferation and cell survival. In this study, the observed RV inhibition of TGF- β -induced Akt phosphorylation may explain the antiproliferative effect following RV treatment. In contrast, RV did not have any effect on Akt signaling in rat cardiac fibroblasts, at least under basal conditions [24]. However, RV treatment of VSMCs inhibited phosphorylation of PI3K, which is directly upstream from Akt [36]. Therefore, our results highlight important cell-specific differences that are attributed to the inhibitory actions of RV.

Finally, supporting previous results reported from analysis of MCF7 cells [37], our data demonstrate that RV treatment partially restored the TGF-

β -mediated reduction of PTEN mRNA and protein levels. On the other hand, in lung biopsy samples from IPF/UIP patients, α -SMA expression is observed only in fibroblasts which demonstrate inhibition or loss of PTEN activity. Moreover, in a mouse model, inhibition of PTEN activity is both necessary and sufficient to induce myofibroblast differentiation whereas PTEN overexpression suppresses α -SMA expression, cell proliferation, and collagen production in myofibroblasts [12].

CONCLUSIONS

RV has already been shown to exert cardioprotective, cholesterol-lowering, and antiatherosclerotic

properties. This study now provides direct evidence demonstrating that RV can also inhibit 2 critical stages of human lung fibroblast activation in the fibrotic process: proliferation and differentiation into myofibroblasts. Because both of these pathophysiological parameters are key determinants of lung fibrosis, RV might be proposed as a potential adjuvant in the treatment of IPF/UIP. Moreover, RV could be very effective in alleviating fibrotic side effect of bleomycin chemotherapeutic agent.

Declaration of interest: The authors report no conflicts of interest. The authors alone are responsible for the content and writing of the paper.

REFERENCES

- [1] Hinz B, Phan SH, Thannickal VJ, Galli A, Bochaton-Piallat ML, Gabbiani G: The myofibroblast: one function, multiple origins. *Am J Pathol.* 2007;170:1807–1816.
- [2] Gabbiani G: The myofibroblast in wound healing and fibrocontractive diseases. *J Pathol.* 2003;200:500–503.
- [3] Phan SH, Zhang K, Zhang HY, Gharaee-Kermani M: The myofibroblast as an inflammatory cell in pulmonary fibrosis. *Curr Top Pathol.* 1999;93:173–182.
- [4] Serini G, Bochaton-Piallat ML, Ropraz P, Geinoz A, Borsi L, Zardi L, Gabbiani G: The fibronectin domain ED-A is crucial for myofibroblastic phenotype induction by transforming growth factor-beta1. *J Cell Biol.* 1998;142:873–881.
- [5] Phan SH: The myofibroblast in pulmonary fibrosis. *Chest.* 2002;122:286S–289S.
- [6] Raghu G, Masta S, Meyers D, Narayanan AS: Collagen synthesis by normal and fibrotic human lung fibroblasts and the effect of transforming growth factor-beta. *Am Rev Respir Dis.* 1989;140:95–100.
- [7] Ramos C, Montano M, Garcia-Alvarez J, Ruiz V, Uhal BD, Selman M, Pardo A: Fibroblasts from idiopathic pulmonary fibrosis and normal lungs differ in growth rate, apoptosis, and tissue inhibitor of metalloproteinases expression. *Am J Respir Cell Mol Biol.* 2001;24:591–598.
- [8] Fine A, Goldstein RH: The effect of transforming growth factor-beta on cell proliferation and collagen formation by lung fibroblasts. *J Biol Chem.* 1987;262:3897–3902.
- [9] Caraci F, Gili E, Calafiore M, Failla M, La RC, Crimi N, Sortino MA, Nicoletti F, Copani A, Vancheri C: TGF-beta1 targets the GSK-3beta/beta-catenin pathway via ERK activation in the transition of human lung fibroblasts into myofibroblasts. *Pharmacol Res.* 2008;57:274–282.
- [10] Hashimoto S, Gon Y, Takeshita I, Matsumoto K, Maruoka S, Horie T: Transforming growth factor-beta1 induces phenotypic modulation of human lung fibroblasts to myofibroblast through a c-Jun-NH2-terminal kinase-dependent pathway. *Am J Respir Crit Care Med.* 2001;163:152–157.
- [11] Fang LP, Lin Q, Tang CS, Liu XM: Hydrogen sulfide suppresses migration, proliferation and myofibroblast transdifferentiation of human lung fibroblasts. *Pulm Pharmacol Ther.* 2009;22:554–561.
- [12] White ES, Atrasz RG, Hu B, Phan SH, Stambolic V, Mak TW, Hogaboam CM, Flaherty KR, Martinez FJ, Kontos CD, Toews GB: Negative regulation of myofibroblast differentiation by PTEN (Phosphatase and Tensin Homolog Deleted on chromosome 10). *Am J Respir Crit Care Med.* 2006;173:112–121.
- [13] Horowitz JC, Rogers DS, Sharma V, Vittal R, White ES, Cui Z, Thannickal VJ: Combinatorial activation of FAK and AKT by transforming growth factor-beta1 confers an anoikis-resistant phenotype to myofibroblasts. *Cell Signal.* 2007;19:761–771.
- [14] Xia H, Diebold D, Nho R, Perlman D, Kleidon J, Kahm J, Avdulov S, Peterson M, Nerva J, Bitterman P, Henke, C: Pathological integrin signaling enhances proliferation of primary lung fibroblasts from patients with idiopathic pulmonary fibrosis. *J Exp Med.* 2008;205:1659–1672.
- [15] Walter N, Collard HR, King TE Jr: Current perspectives on the treatment of idiopathic pulmonary fibrosis. *Proc Am Thorac Soc.* 2006;3:330–338.
- [16] Nathan SD: 2006. Therapeutic management of idiopathic pulmonary fibrosis: an evidence-based approach. *Clin Chest Med.* 2006;27:S27–S35, vi.
- [17] Sener G, Topaloglu N, Schirli AO, Ercan F, Gedik, N: Resveratrol alleviates bleomycin-induced lung injury in rats. *Pulm Pharmacol Ther.* 2007;20:642–649.
- [18] Zhou M, He JL, Yu SQ, Zhu RF, Lu J, Ding FY, Xu GL: [Effect of resveratrol on chronic obstructive pulmonary disease in rats and its mechanism]. *Yao Xue Xue Bao.* 2008;43:128–132.
- [19] Aggarwal BB, Bhardwaj A, Aggarwal RS, Seeram NP, Shishodia S, Takada, Y: Role of resveratrol in prevention and therapy of cancer: preclinical and clinical studies. *Anticancer Res.* 2004;24:2783–2840.
- [20] Granados-Soto V: Pleiotropic effects of resveratrol. *Drug News Perspect.* 2003;16:299–307.
- [21] Sgambato A, Ardito R, Faraglia B, Boninsegna A, Wolf FI, Cittadini, A: Resveratrol, a natural phenolic compound, inhibits cell proliferation and prevents oxidative DNA damage. *Mutat Res.* 2001;496:171–180.
- [22] Ignatowicz E, Baer-Dubowska W: Resveratrol, a natural chemopreventive agent against degenerative diseases. *Pol J Pharmacol.* 2001;53:557–569.
- [23] Burstein B, Maguy A, Clement R, Gosselin H, Poulin F, Ethier N, Tardif JC, Hebert TE, Calderone A, Nattel S: Effects of resveratrol (trans-3,5,4'-trihydroxystilbene) treatment on cardiac remodeling following myocardial infarction. *J Pharmacol Exp Ther.* 2007;323:916–923.
- [24] Olson ER, Naugle JE, Zhang X, Bomser JA, Meszaros JG: Inhibition of cardiac fibroblast proliferation and myofibroblast differentiation by resveratrol. *Am J Physiol Heart Circ Physiol.* 2005;288:H1131–H1138.
- [25] Jordana M, Schulman J, McSharry C, Irving LB, Newhouse MT, Jordana G, Gaudie J: Heterogeneous proliferative characteristics of human adult lung fibroblast lines and clonally derived fibroblasts from control and fibrotic tissue. *Am Rev Respir Dis.* 1988;137:579–584.
- [26] Conte E, Nigro L, Fagone E, Drago F, Cacopardo B: Quantitative evaluation of interleukin-12 p40 gene expression in peripheral blood mononuclear cells. *Immunol Invest.* 2008;37:143–151.
- [27] Wang Z, Chen Y, Labinskyy N, Hsieh TC, Ungvari Z, Wu JM: Regulation of proliferation and gene expression in cultured human aortic smooth muscle cells by resveratrol and standardized grape extracts. *Biochem Biophys Res Commun.* 2006;346:367–376.
- [28] Jordana M, Schulman J, McSharry C, Irving LB, Newhouse MT, Jordana G, Gaudie J: Heterogeneous proliferative characteristics of human adult lung fibroblast lines and clonally derived fibroblasts from control and fibrotic tissue. *Am Rev Respir Dis.* 1988;137:579–584.
- [29] Raghu G, Chen YY, Rusch V, Rabinovitch PS: Differential proliferation of fibroblasts cultured from normal and fibrotic human lung. *Am Rev Respir Dis.* 1988;138:703–708.

- [30] Raghu G, Masta S, Meyers D, Narayanan AS: Collagen synthesis by normal and fibrotic human lung fibroblasts and the effect of transforming growth factor- β . *Am Rev Respir Dis.* 1989;140:95–100.
- [31] Godichaud S, Krisa S, Couronne B, Dubuisson L, Merillon JM, Desmouliere A, Rosenbaum J: Deactivation of cultured human liver myofibroblasts by trans-resveratrol, a grapevine-derived polyphenol. *Hepatology.* 2000;31:922–931.
- [32] Le Corre L, Chalabi N, Delort L, Bignon YJ, Bernard-Gallon DJ: Differential expression of genes induced by resveratrol in human breast cancer cell lines. *Nutr Cancer.* 2006;6:193–203.
- [33] Hu Y, Peng J, Feng D, Chu L, Li X, Jin Z, Lin Z, Zeng Q: Role of extracellular signal-regulated kinase, p38 kinase, and activator protein-1 in transforming growth factor-beta1-induced alpha smooth muscle actin expression in human fetal lung fibroblasts in vitro. *Lung.* 2006;184:33–42.
- [34] Haider UG, Sorescu D, Griendling KK, Vollmar AM, Dirsch VM: Resveratrol suppresses angiotensin II-induced Akt/protein kinase B and p70 S6 kinase phosphorylation and subsequent hypertrophy in rat aortic smooth muscle cells. *Mol Pharmacol.* 2002;62:772–777.
- [35] Martin MM, Buckenberger JA, Jiang J, Malana GE, Knoell DL, Feldman DS, Elton TS: TGF-beta1 stimulates human AT1 receptor expression in lung fibroblasts by cross talk between the Smad, p38 MAPK, JNK, and PI3K signaling pathways. *Am J Physiol Lung Cell Mol Physiol.* 2007;293:L790–L799.
- [36] Haider UG, Sorescu D, Griendling KK, Vollmar AM, Dirsch VM: Resveratrol suppresses angiotensin II-induced Akt/protein kinase B and p70 S6 kinase phosphorylation and subsequent hypertrophy in rat aortic smooth muscle cells. *Mol Pharmacol.* 2002;62:772–777.
- [37] Waite KA, Sinden MR, Eng C: Phytoestrogen exposure elevates PTEN levels. *Hum Mol Genet.* 2005;14:1457–1463.